University of Baghdad
College of Engineering
JOURNAL OF ENGINEERING

Journal of Engineering

journal homepage: www.joe.uobaghdad.edu.iq

Volume 29 Number 2 February 2023

Study the Effect of Adding Aluminum Nanoparticles to a Smart Alloy (Cu-Al-Ni) on Hardness and Porosity

Myasar Abdulkareem Mohammed Jaffar *
MSc. student
College of Engineering – University of Baghdad
Iraq, Baghdad
myasar.jaffar2003m@coeng.uobaghdad.edu.iq

Ahmed Abdulrasool Ahmed Alkhafaji
Prof. Dr.
College of Engineering – University of Baghdad
Iraq, Baghdad
dr.ahmed.a.ahmed@coeng.uobaghdad.edu.iq

ABSTRACT

This work deals with the effect of adding aluminum nanoparticles on the mechanical properties, micro-hardness, and porosity of memory-shaped alloys (Cu-Al-Ni). These alloys have wide applications in various industrial fields such as (high damping compounds and self-lubricating applications). The samples are manufactured using the powder metallurgy method, which involved pressing in only one direction and sintered in a furnace surrounded by an inert gas. Four percentages (0%, 5%, 10%, and 15%) of aluminum nanoparticles were fabricated, which depended on the weight of aluminum powder (13%) in the sample under study.

To find out which phase is responsible for the reliability of the formation of this type of alloy and its porosity, X-ray diffraction (XRD) and scanning electron microscopy (SEM) tests are used. The Vickers micro-hardness and porosity properties of these alloys were studied using a Vickers micro-hardness and porosity tester according to ASTM b328-1996.

The results showed that increasing the concentration of aluminum nanoparticles in the alloy led to an increase in hardness with a decrease in porosity, and the sample (15%) gave the best hardness (190.8 HV). The sample (0%) gave the highest porosity (19.573) %.

Keywords: (Cu-Al-Ni) smart alloys, powder metallurgy, hardness, porosity.

*Corresponding author
Peer review under the responsibility of University of Baghdad.
https://doi.org/10.31026/j.eng.2023.02.01
This is an open access article under the CC BY 4 license(http://creativecommons.org/licenses/by/4.0/).
Article received: 11/6/2022
Article accepted: 3/9/2022
Article published: 1/2/2023

دراسة تأثير إضافة جسيمات الألمنيوم النانوية على الصلادة والمسامية لسبيكة (Cu-Al-Ni) الذكية

ميسر عبد الكريم محمد جعفر
طالب ماجستير
جامعة بغداد/كلية الهندسة

أحمد عبد الرسول أحمد
أستاذ دكتور
جامعة بغداد/كلية الهندسة

الخلاصة

تناول هذا العمل تأثير إضافة جزيئات الألمنيوم النانوية على الخواص الميكانيكية ، الصلادة الدقيقة والمسامية لسبائك متذكرة الشكل (Cu-Al-Ni). لهذه السبائك تطبيقات واسعة في مختلف المجالات الصناعية مثل (مركبات التخميد العالية وتطبيقات التشحيم الذاتي). طريقة التصنيع للعينات كانت باستخدام طريقة تعدين المساحيق ، والتي تضمنت الضغط في اتجاه واحد فقط ، ومبلدة في فرن محاط بغاز خامل. تم تصنيع أربع نسب (0٪ ، 5٪ ، 10٪ ، 15٪) من جسيمات الالمنيوم النانوية والتي أعتمد على نسبة وزن مسحوق الألمنيوم (١٣%) في العينة قيد الدراسة.

لمعرفة المرحلة المسؤولة عن موثوقية تشكيل هذا النوع من السبائك والمسامية ، استخدم فحص حيود الأشعة السينية (XRD)، وفحص المجهر الإلكتروني (SEM). تمت دراسة خصائص فيكرز للصلادة الدقيقة والمسامية لهذه السبائك باستخدام جهاز فيكرز للصلادة الدقيقة وفحص المسامية وفقًا لـ ASTM b328-1996. أظهرت النتائج أن زيادة تركيز جزيئات الالمنيوم النانوية في السبيكة أدى إلى زيادة الصلادة مع أنخفاض المسامية، وقد أعطت العينة (١٥%) أفضل صلادة (HV 190.8) . وأعطت العينة (٠%) أعلى مسامية (19.573)٪.

الكلمات الرئيسية : (Cu-Al-Ni) سبائك ذكية ، ميتالورجيا المساحيق ، صلادة ، مسامية.

1. INTRODUCTION

Shape memory alloys (SMAs) are materials with the ability to revert to their original shape when their temperature increases above their transformation point due to various environmental factors, even after severe plastic deformations **[Jasim, et al., 2021].** When their temperature falls below their transition point, they have very low yield strength and may be easily bent into any desired shape, which they will maintain **[Hautcoeur, et al., 2015]**. Because of the SMAs' distinctive properties, they have gained significant economic and technological relevance, and they are now used in a wide range of applications, including medical, industrial, and aerospace applications **[Kolekar, et al., 2017]**. The thermoplastic martensitic transition, a particular reversible crystalline transformation, is the foundation of SMAs' distinctive features **[Qasim, et al., 2022]**. The martensitic transformation occurs between two solid phases: the first, called austenite (a parent phase), is stable at high temperatures and has a body-centered cubic crystal structure (BCC) with a face-centered

tetragonal cell within the BCC structure, and the second, called (twinned or DE twinned) martensitic (a product phase), is stable at low temperatures and has a (tetragonal, monoclinic) crystal structure in the Ni-Ti alloys **[Hussain, et al., 2017]**. The goal of this research is to find out how the concentration ratio of Al nanoparticles to the hardness and porosity of (Cu-Al-Ni) smart alloys.

(Ahmed and Hasan, 2017): To make a form memory alloy Powder metallurgy was employed to make Cu-13 percent Al-4 percent Ni alloy in this investigation, with five samples sintered at different sintering times (3,4,5,6,7) hours each. The Martensite phase was also stabilized by heating the samples. Shape recovery & the porosity results were analyzed utilizing an Artificial Neural Network (ANN) forecasting method which anticipates the shape recovery and porosity conduct among (3) and (7) hrs., because, no link between porosity & shape recovery on a physical level.

(Ahmed and Bassam 2018): The influence of Cu and AL of the (Cu Al Ni) respecting a physical and mechanical difference for the smart alloy (Cu Al Ni), created by Powder Metallurgy Method at a steady weight ratio of (Ni) in each of the proportions is studied in this work. Each created sample has the same compacting pressure and sintering temperature. The maximum value of microhardness is 185HV, according to the findings of the sample test, which occurred in weight percentage (82Cu, 14Al, 4Ni) %.

(Taher and Ahmed 2018): The newly obtained results in this study selected the optimum ratio in (Cu Al Ni) alloys by studying the concentration of (Cu Ni) & (Al Ni), The newly obtained results in this study selected the optimum proportion in (Cu Al Ni) alloys by study the concentration effect of (Cu Ni) & (Al Ni) with used five different weight ratios of these concentrations, and produced the better hardness and porosity. Powder metallurgy and a vacuum apparatus were used to create the (Cu-Al-Ni) smart alloy samples. The effects of (Cu-Ni) and (Al-Ni) concentration ratios on hardness and porosity of (Cu-Al-Ni) smart alloy were studied using the Vickers Micro-Hardness unit and porosity experiment according to ASTM b328-(1996). The findings of the investigation demonstrated that showed that increasing the Al and Ni concentrations in an alloy, increases hardness & porosity.

(Raed and Razooqi, 2020): In this work Powder Metallurgy was used to create a Cu-Al-Ni alloy and the other alloy by adding the alloying elements (Mg) with the content of (0.25, 0.5, 0.75, 1.0, 1.25) % by mixing powder for speed (20 rpm), and (16 min) respectively. 500 MPa was compacting and 900˚ C was sintering for one hr. The results showed that both bulk density and apparent density compared to the base alloy increased by increasing the volumetric fraction of Mg by the ratios (5.49) % compared to the bulk density of the base alloy and by the ratios (1.51) % compared to the apparent density of the base alloy. Decrease in the real and apparent porosity and water absorption. The results of the mechanical tests showed an increase in the hardness and diametrical compressive strength with the increase of the volumetric fraction of (Mg) compared to the base alloy.

2. THEORETICAL CONSIDERATIONS

The manufacturing method involved four stages of (Cu-Al-Ni) alloy:

- Mixing process.

The goal of mixing is to obtain good powder homogeneity. The greatest results are obtained when the container is between 20% and 40% filled. Then, during this process, several materials are added, such as tiny lubricants (zinc and aluminum stearates) to reduce friction during mixing and compaction deflocculates to avoid powder agglomeration and improve flow characteristics for subsequent operations.

- Compacting process

According to the number of punches utilized in the process, the compressing procedure can be divided into many types:
One-direction compressing when using one punch.
Two opposite directions compressing by using two punches. **(Groover, 2013).**

- Sintering process.

Also known as solid-state sintering is a heat treatment performed on green compact in an atmospheric furnace at temperatures between 0.7 and 0.9 degrees Celsius over the melting temperature of the material, the goal of this technique is to bind the alloy particles together using a plastic and diffusion flow mechanism, resulting in increased strength and hardness **[Taher and Ahmed, 2018]**. **Fig. 1** shows the sintering process steps.

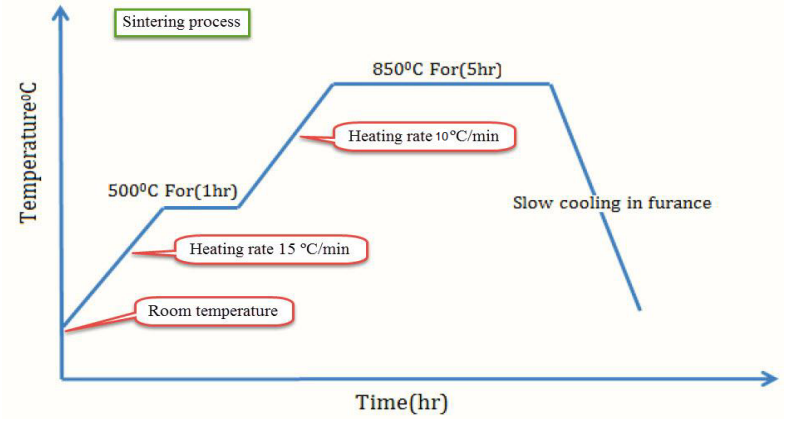

Figure 1. Diagram of sintering process steps

- Heat treatment

The heating and cooling procedures that are performed on the material are referred to as heat treatment. In this study, two forms of heat treatment were used: quenching and aging procedures. These techniques are used to obtain the Austenite phase by aging and the martensitic phase by quenching **[Hasan, 2016]**. **Fig.2** shows the heat treatment process steps.

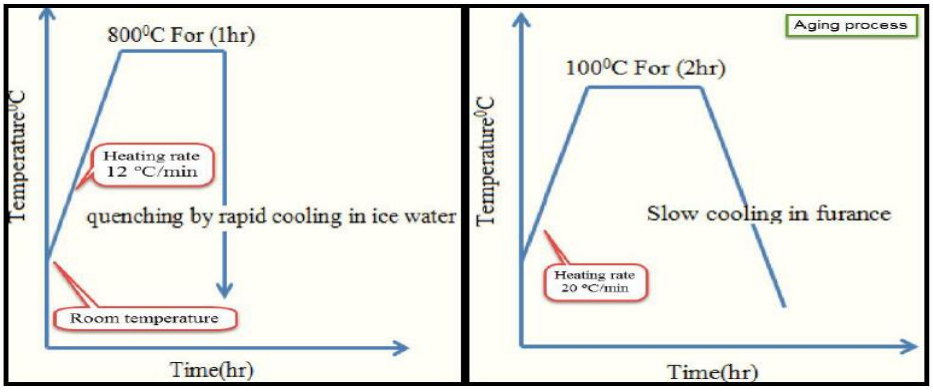

Figure 2. Diagram of heat treatment process steps

a. Hardness

Hardness tests are performed using various materials and shapes of load, such as Vickers, Rockwell, Brinell, and Knoop tests, to determine how resistant a surface material is to wear and scratch. The Vickers micro-hardness test is used to determine the hardness of very thin or very small materials using loads ranging from 1 to 1000 gm **[Taher and Ahmed, 2018]**. This test was used in this research because smart alloy applications such as actuators, sensors, and wires are frequently subjected to very light loads and very small sizes.

b. Porosity

There are two types of pores: (a) external spaces between alloy particles known as open pores, through which liquids such as oil, molten materials, and water penetrate the internal alloy structure to achieve the properties of a special new alloy that can be used in a variety of applications such as filters, dampers, and self-lubrication applications; and (b) internal spaces in the body of single-particle alloys. The closed pores have a minor effect and a modest volume. The open pores of the alloy can be computed, and the resulting value represents the alloy's apparent porosity, which is impacted by factors such as compacting pressure, chemical composition, and heat treatment. As Eq. (1) **(Shafeeq, et al., 2016)**

$$p = \left(\frac{(B-A)*100}{(B-F)*\boldsymbol{Do}}\right) * Dw \qquad (1)$$

P = Porosity by volume, %.
A = Mass in air gm.
B = Mass of the oil-impregnated specimen, gm.
F = Mass of the oil-impregnated sample in water with wire tarred mass, g.
Dw= Density of water, (0.9984 gm/cm^3).
Do= Density of oil, 0.88 gm/cm^3

3. EXPERIMENTAL WORK

The following techniques were used to experiment:

- The pure powders of (Cu 99.9%, Al 99% & Ni99.5%) purity with an average particle size of 44 microns (-325 mesh) were purchased from general Drag House Company/ India, and Aluminum nanoparticles with a purity of 99.9% and particle size of 40nm which production by Hongwu international group/ china.
- Using the powder technique that was mentioned on the theoretical side. Eight cylindrical samples (5mm thickness and 11mm diameter). It was formed through the following step: As shown in **Table 1**.

a) To combine the materials, a 3-digit sensitive balance and a revolving drum mixer device were used to mix the particles (Cu, Al, Ni) (S1, S2, S3, S4) before adding the nanoparticles for 6 hours. The mixture was placed in the glass container at 40% of its volume to achieve the best mixing results, with 1% acetone added to avoid particle segregation (because of the varying densities of the alloying components) and for lubrication. The second stage is to divide the samples into (3 gm) weight groups, then add nanoparticles and re-mix each sample using a manual mixing bowl. **Fig.3** shows the samples before mixing.

Table 1. Distribution of weight for materials

No. of sample	Cu (83%)	Al (13%)	Ni (4%)	Nanoparticle (gm)	Qty. of samples	sample weight (gm)
S1	2.49	0.39	0.12	0	2	3
S2				0.019		3.019
S3				0.039		3.039
S4				0.058		3.058

Figure 3. The samples before mixing

b) The dimensions of dies (D_o* D_{in}*L)=(46*11.2*65) mm to fabricate the (Cu-Al-Ni) SMAs samples, the dimensions of first punch (D* L)=(11*80) mm (move in one direction) and the second punch (fixed) (D*L) =(11*20) mm which they used to compact the samples in die. To increase the accuracy, two samples were made for each concentration, and then the average value was taken in the reading for the hardness and porosity.

c) An electrical uniaxial press machine with a load capacity of 100 kN was used to compact all of the samples in one direction to achieve the necessary component shape (D*t) = (11*5 mm) at constant pressure 650 MPa with a displacement rate of 1 mm/min and a holding time for two minutes**. Fig. 4** shows the electrical uniaxial press machine, dies, and punches.

Figure 4. The electrical uniaxial press machine dies and punches.

d) The sintering process was divided into two parts, with the first stage occurring at a constant temperature of 500°C for one hour and the second stage occurring at a constant temperature of 850°C for five hours. An electrical tube furnace was used with an inert gas system (Argon gas) to avoid oxidation of the samples to achieve solid-state bonding of the particles and strengthening of the component. **Fig. 5** shows the electrical furnace with an inert gas system and samples after sintering.

Figure 5. Electrical furnace with inert gas system and samples after sintering.

e) Heat treatment was done in two stages. The quenching procedure involves heating to 800°C for one hour, then rapidly cooling through ice water to achieve the martensitic phase. The aging process involves heating to 100°C for two hours, then cooling in the furnace to achieve martensitic stabilization.

4. The EXAMINATIONS

4.1. Physical Examinations

Physical tests are performed after the heat treatment, grinding, polishing, and etching to observe the pores, granule boundaries, and types of the subsequent phases. These tests are classified as non-destructive material testing. **Fig. 6** shows the grinding, polishing, and etching. Scanning Electron Microscope (SEM) **Fig. 7.** And X-ray Diffraction Test (XRD) **Fig. 8**

Figure 6. Grinding, polishing, and etching

Figure 7. Scanning Electron Microscope device

Figure 8. X-Ray Diffraction device

4.2. Mechanical Examination

4.2.1. Hardness

To explore the influence of nanoparticle addition of smart alloys respecting Hardness, Vickers micro-hardness testing was performed, an examination was conducted on eight samples divided into two groups, and the average was taken between every two samples. The micro-hardness device was used at 400 gm load and a holding duration time of 20 seconds **[Taher and Ahmed, 2018]**. **Fig. 9** Shows the Digital Vickers micro-hardness.

Figure 9. Vickers micro-hardness

4.2.2. Porosity

Use a sensitive balance (3 digits) to weigh each weight percentage of samples in three separate scenarios to conduct porosity testing on eight samples. The examination was conducted on eight samples divided into two groups, and the average was taken between every two samples. The first is that it should be weighed in the air, the second is that it should be immersed in a closed container containing oil (0.88 g\cm^3) and vacuumed for 30 minutes at room temperature inside the closed container, and the third is that it should be opened and set aside for ten minutes before being weighed in the air after cleaning the sample of excess oil. The oil-soaked sample should be weighed in water using a bin with a hock in the third condition. **Fig. 10** shows the porosity testing **[Taher and Ahmed, 2018]**.

Figure 10. Porosity testing

5. RESULTS AND DISCUSSION

- **Fig. 11**: SEM images of specimens after heat treatment. The Martensite phase was visible in all specimens with martensitic layers, generated by heat treatment.

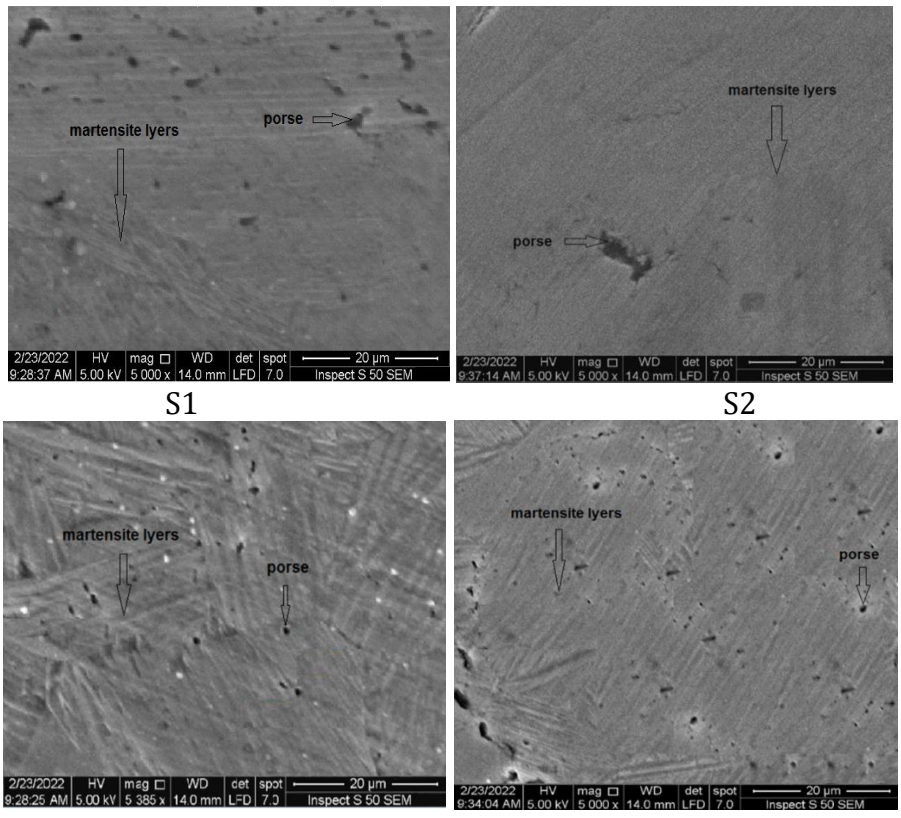

S1 S2

S3 S4

Figure 11. Scanning Electron Microscope examination

- **Fig. 12**: XRD showing the formation of the martensite phase following sintering and heat treatment. The martensite behavior is depicted in **Fig. 1**. XRD peaks will not appear, if it is less than 5%, which the proportion of Ni is 4%, Its intensity will be low compared to the percentage of the element in the alloy, and the fewer intensity peaks cannot be observed in the pattern if the other compound is highly crystalline possess high intense XRD peaks. Then Ni peaks will exist but due to the high intensity of other compounds, they cannot be observed **(Cullity, 1987)**.

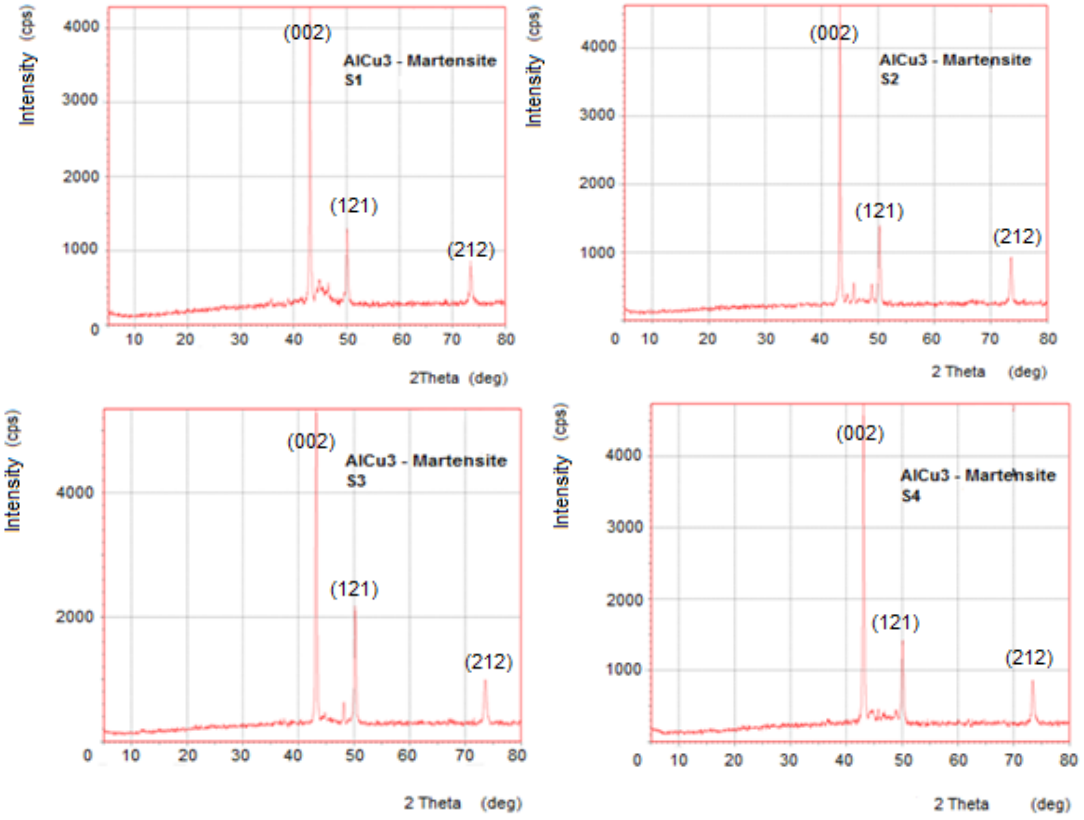

Figure 12. X-Ray Diffraction Examinations

- **Table 2** shows the Vickers micro-hardness test on specimens. The examination was performed on eight samples separated into two groups, with the average selected from each pair of specimens. Three micro-hardness spots on the surface of the specimens were measured; observe the variation in readings for one specimen. Because of the likelihood of measuring on zone having porosity. The mean is used as a criterion for scoring.

Table 2. Vickers micro-hardness test.

Sample No.	chemical composition	HV1		HV2		HV3		HV(Average)		Final HV (Average)
S1	83%Cu, 13%Al, 4%Ni without nanoparticle	130.9	122.4	125.4	133.7	151.3	140.5	135.8	132.2	134
S2	83%Cu, 13%Al, 4%Ni with 5% Al nanoparticle	166.7	159.2	158.6	167.9	170.9	166.3	165.4	164.4	164.9
S3	83%Cu, 13%Al, 4%Ni with 10% Al nanoparticle	182.6	177.2	175.4	181.6	185.7	180.2	181.2	179.6	180.4
S4	83%Cu, 13%Al, 4%Ni with 15% Al nanoparticle	192.6	195.6	188.5	193.5	191.4	189.7	190.8	192.9	191.8

- **Fig. 13** presents the results for the measurement of the Vickers micro-hardness which showed an increase with an increase in nanoparticles, The average value of the hardness is at the base sample (Sd1) (134 HV) It is the lowest value. While it increased by (30.9 %), as the average value (164.9 HV) for the second sample (Sd2). The third sample (Sd3), increase from the base sample by (46.4%), and about the second sample (15.5%), as the average value (180.4 HV), The fourth sample (Sd4) increased from the base sample (Sd1) by (57.8%), about the second sample (Sd2) (26.9%), and about the third sample (Sd3) (11.4%) as the average value (191.8 HV).

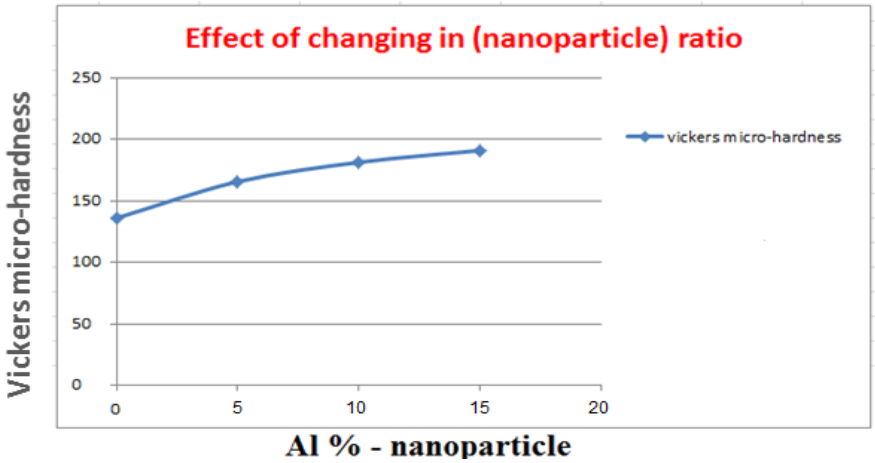

Figure 13. The graph shows the effect of changing in (Al nanoparticle %) ratio on Vickers micro-hardness in (Cu-Al-Ni) smart alloys.

- **Table 3** shows the results of porosity tests on samples. The test was performed on eight samples separated into two groups, with the average selected from each pair of samples. This is to increase the accuracy of the results, as it is not possible to depend on a single sample result.

Table 3. Porosity Results.

Sample No.	chemical composition	A (gm) in Air		B (gm) in oil		F(gm) in water		Porosity %		Final Porosity %
S1	83%Cu, 13%Al, 4%Ni without nanoparticle	2.859	2.864	2.962	2.995	2.370	2.346	19.573	22.708	21.140
S2	83%Cu, 13%Al, 4%Ni with 5% Al nanoparticle	2.930	2.849	3.033	2.943	2.393	2.412	18.105	19.915	19.01
S3	83%Cu, 13%Al, 4%Ni with 10% Al nanoparticle	2.860	2.822	2.906	2.892	2.317	2.107	8.404	10.031	9.217
S4	83%Cu, 13%Al, 4%Ni with 15% Al nanoparticle	2.755	2.812	2.774	2.853	2.169	1.148	3.533	2.732	3.132

- **Fig. 14** shows the results for the measurement of porosity which showed a decrease with an increase in (Al) nanoparticles, the average value of the porosity (Sd1) is (21.140), which is the highest value. While it decreased by (2.13%), as the average value (19.01) for the second sample (Sd2). The third sample (Sd3), declined from the base sample (Sd1) by (11.923%), and the second sample by about (9.793%), as the average value (9.217), the fourth sample (Sd4) decreased from the base sample (Sd1) by (18.008%), the second sample (Sd2) about (15.878%), and the third sample (Sd3) about (6.085%) as the average value (3.132).

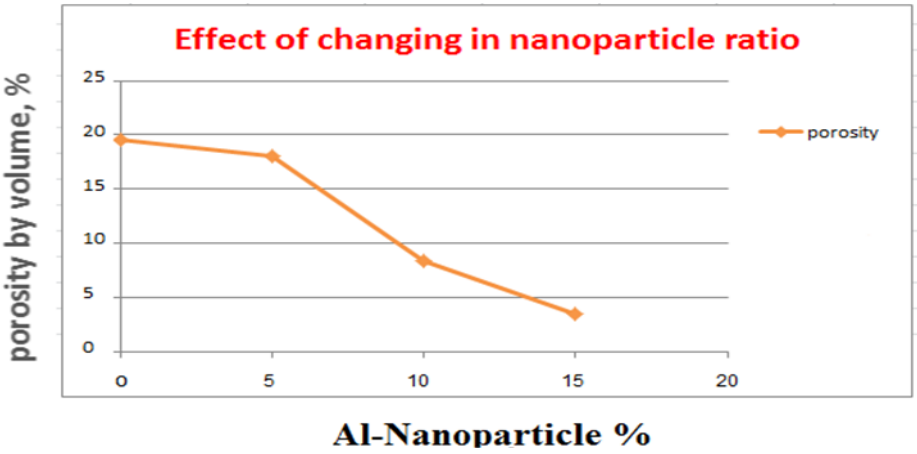

Figure 14. The graph shows the effect of changing in (Al nanoparticle %) ratio on porosity % in (Cu-Al-Ni) smart alloys.

6. CONCLUSION

- Each sample was mixed separately to ensure a homogeneous distribution of nanoparticles within the sample as much as possible so as not to occur segregation of materials and this leads to different physical and mechanical properties
- The reason for the difference in the weights of the samples is that the addition was made with the stability of the basic weight of the original powder elements.
- In the hardness test of the samples under study, the rise in the percentage of nanoparticle addition increases the microscopic hardness.
- The porosity test showed a different behavior from the hardness test, where the porosity increased when no nanoparticles were added.

REFERENCES

Ahmed, A., and Bassam, S., 2018. Effect of Cu-Al Proportions in Smart (Cu-Al-Ni) Alloy for Best Mechanical properties by Using Artificial Intelligent., Association of Arab Universities Journal of Engineering Sciences, 1 (25).

Ahmed, A., and Hasan, A., 2017. Investigation on Relationship between Shape Memory Effect and Interconnection Porosity under Multiple Sintering Time of Smart Alloy Cu-Al-Ni., Association of Arab Universities Journal of Engineering Sciences, 3 (24).

Cullity, B., 1987. Elements of X-ray Diffraction Addison-Wesley series in metallurgy and materials. United States of America, University of Michigan.

Groover, M., 2013. Fundamentals of Modern Manufacturing Materials, Processes, and Systems. United States of America, Lehigh University.

Hasan, A., 2016. Prediction of Mechanical Properties of Smart Alloy Cu-Al-Ni based on Sintering Time by Using ANN., College of Engineering of Baghdad University.

Hautcoeur, A., Fouché, F. and Sicre, J., 2016, May. Cu-Al-Ni shape memory single crystal wires with high transformation temperature. In *43rd Aerospace Mechanisms Symposium*, May, pp. 185-191.

Kolekar, A., Natak, A., Navratne, K. and Mali, A., 2017. Recent advancement in shape memory alloy. *International Research Journal of Engineering and Technology (IRJET)*, *4*(4), pp.2120-2125.

Qasim, M. F., Abbas, Z.K., Abed, S. K., 2022. Production of Load Bearing Concrete Masonry Units (blocks) From Green Concrete Containing Plastic Waste and Nano Silica Sand Powder., Journal of Engineering, 28(8), 54-70.

Jasim, N.A.H., Shafiqu, Q.S. and Ibrahim, M.A., 2021. The Effect of Adding High-Density Polyethylene Polymer on the Engineering Characteristics for Sandy Soil. *Journal of Engineering*, *27*(9), pp.29-37.

Raed, N., and Razooqi, J., 2020. Influences of Mg Addition on the Mechanical Properties of Cu-Al-Ni Shape Memory Alloys. *Tikrit Journal of Engineering Sciences*, 27(3), 82- 93.

Hussain, S., Jain, A.K., Ansari, M.A., Pendy, A. and Dasgupta, P., 2017. Study of effect of Fe, Cr and Ti on the martensite phase formation in Cu-12, 5wt% Al-5wt% Mn SMA. *Advanced Materials Proceedings*, *2*(1), pp.22-25.

Shafeeq, M.M., Gupta, G.K., Malik, M.M., Sampath, V. and Modi, O.P., 2016. Influence of quenching methods on martensitic transformation and mechanical properties of P/M processed Cu–Al–Ni–Ti shape memory alloys. *Powder Metallurgy*, *59*(4), pp.271-280.

Taher, M., and Ahmed A., 2018. Effect of (Al-Ni) & (Cu-Ni) Concentrations Ratios on the Hardness and Porosity of Ternary (Cu-Al-Ni) Smart Alloys. Australian Journal of Basic and Applied Sciences, 12(2), 36-48.

Taher, M., and Ahmed A., 2018. Study the Mechanical Properties of Ternary (Cu-Al-Ni) Shape Memory Alloys Affected by (Al-Ni) and (Cu-Ni) Contents Enhancement with ANN., College of Engineering of Baghdad University.